This article was downloaded by: *[United States Naval Academy]*
On: *21 January 2009*
Access details: *Access Details: [subscription number 789040243]*
Publisher *Taylor & Francis*
Informa Ltd Registered in England and Wales Registered Number: 1072954 Registered office: Mortimer House, 37-41 Mortimer Street, London W1T 3JH, UK

Biofouling
Publication details, including instructions for authors and subscription information:
http://www.informaworld.com/smpp/title~content=t713454511

Three Models to Relate Detachment of Low Form Fouling at Laboratory and Ship Scale

M. P. Schultz [a]; J. A. Finlay [b]; M. E. Callow [b]; J. A. Callow [b]
[a] Department of Naval Architecture and Ocean Engineering, United States Naval Academy, Annapolis, MD 21402, USA. [b] School of Biosciences, The University of Birmingham, Birmingham B15 2TT, UK.

First Published on: 01 January 2003

To cite this Article Schultz, M. P., Finlay, J. A., Callow, M. E. and Callow, J. A.(2003)'Three Models to Relate Detachment of Low Form Fouling at Laboratory and Ship Scale',Biofouling,19:1,17 — 26
To link to this Article: DOI: 10.1080/0892701031000089516
URL: http://dx.doi.org/10.1080/0892701031000089516

PLEASE SCROLL DOWN FOR ARTICLE

Full terms and conditions of use: http://www.informaworld.com/terms-and-conditions-of-access.pdf

This article may be used for research, teaching and private study purposes. Any substantial or systematic reproduction, re-distribution, re-selling, loan or sub-licensing, systematic supply or distribution in any form to anyone is expressly forbidden.

The publisher does not give any warranty express or implied or make any representation that the contents will be complete or accurate or up to date. The accuracy of any instructions, formulae and drug doses should be independently verified with primary sources. The publisher shall not be liable for any loss, actions, claims, proceedings, demand or costs or damages whatsoever or howsoever caused arising directly or indirectly in connection with or arising out of the use of this material.

Biofouling, 2003 Vol 19 (Supplement), pp 17–26

Downloaded By: [United States Naval Academy] At: 14:25 21 January 2009

Three Models to Relate Detachment of Low Form Fouling at Laboratory and Ship Scale

M P SCHULTZ[a,*], J A FINLAY[b], M E CALLOW[b] and J A CALLOW[b]

[a]*Department of Naval Architecture and Ocean Engineering, United States Naval Academy, Annapolis, MD 21402, USA;* [b]*School of Biosciences, The University of Birmingham, Birmingham B15 2TT, UK*

(Received 11 April 2002; in final form 22 May 2002)

Since fouling-release coating systems do not prevent settlement, various methods to quantify the tenacity of adhesion of fouling organisms on these systems have been offered. One such method is the turbulent channel flow apparatus. The question remains how the results from laboratory scale tests relate to the self-cleaning of a ship coated with a fouling-release surface. This paper relates the detachment strength of low form fouling determined in the laboratory using a turbulent channel flow to the conditions necessary for detachment of these organisms in a turbulent boundary layer at ship scale. A power-law formula, the ITTC-57 formula, and a computational fluid dynamics (CFD) model are used to predict the skin-friction at ship scale. The results from all three methods show good agreement and are illustrated using turbulent channel flow data for sporelings of the green macrofouling alga *Enteromorpha* growing on a fouling-release coating.

Keywords: adhesion strength; turbulent channel flow; shear stress; microfouling; fouling-release coatings; *Enteromorpha*; biofouling

NOMENCLATURE

A	surface area
a,b	channel flow calibration constants
C_F	friction resistance coefficient $= \frac{F_D}{\frac{1}{2}\rho U_\infty^2 S}$
c_f	local skin–friction coefficient $= \frac{\tau_w}{\frac{1}{2}\rho U_e^2}$
C_p	coefficient of pressure $= \frac{(p-p_\infty)}{\frac{1}{2}\rho U_\infty^2}$
f	channel friction factor
$\vec{F}_D$	frictional drag
$\vec{F}_{CV}$	forces on control volume
H	channel height
k	roughness or organism height
k^+	roughness Reynolds number $= \frac{kU_\tau}{\nu}$
L	length of plate or ship
$\vec{n}$	unit normal vector
p	static pressure
p_∞	static pressure upstream of body
Re_H	channel Reynolds number $= \frac{\bar{U}H}{\nu}$
Re_L	plate or ship Reynolds number $= \frac{U_\infty L}{\nu}$
Re_x	local Reynolds number $= \frac{U_\infty x}{\nu}$
S	wetted surface area
U	local mean velocity
$\bar{U}$	bulk mean velocity in channel
U_e	velocity at the boundary layer edge
U_τ	friction velocity $= \sqrt{\frac{\tau_w}{\rho}}$
U_∞	freestream velocity
U^+	non-dimensional velocity $= \frac{U}{U_\tau}$
$\vec{V}$	fluid velocity vector
$\forall$	control volume
x	distance from leading edge
y	distance from the wall
y^+	non-dimensional distance from the wall $= \frac{yU_\tau}{\nu}$
κ	von Kármán constant $= 0.41$
ν	fluid kinematic viscosity
ρ	fluid density
τ_w	wall shear stress

INTRODUCTION

The introduction of non-toxic, fouling-release coating systems as alternatives to traditional biocide based antifoulings has necessitated a change in coating evaluation protocol. Since fouling-release systems do not prevent settlement *per se* (Swain *et al.*, 1998), various methods to quantify the tenacity of adhesion of fouling organisms on these systems have

*Corresponding author; fax: (410) 293-2219; e-mail: mschultz@usna.edu

ISSN 0892-7014 print/ISSN 1029-2454 online © 2003 Taylor & Francis Ltd
DOI: 10.1080/0892701031000089516

Downloaded By: [United States Naval Academy] At: 14:25 21 January 2009

been offered. Among these are the hard fouling adhesion test (ASTM D5618, 1994), the water jet cleaning method (Swain & Schultz, 1996; Finlay *et al.*, 2002), the towed foil technique (Kovach & Swain, 1998) and the turbulent channel flow apparatus (Schultz *et al.*, 2000). Data from these tests are of particular importance because fouling-release surfaces that cannot "self clean" due to hydrodynamic forces or be mechanically cleaned without significant damage will be likely to suffer large drag penalties.

The question remains as to how the results from laboratory scale tests relate to the self-cleaning of a ship coated with a fouling-release surface. The goal of the present research was to relate the detachment strength of low form fouling determined by the turbulent channel flow apparatus to the conditions necessary for detachment of these organisms in a turbulent boundary layer at ship scale. First, the fundamentals of turbulent channel and boundary layer flows are reviewed and their similarities and differences discussed. Three methods for the determination of ship scale skin-friction are then presented. These are related to the conditions in a laboratory turbulent channel flow apparatus using boundary layer similarity laws. Finally, the three models are used to predict detachment at ship scale based on turbulent channel flow data obtained using biofilms of different ages of the green fouling alga *Enteromorpha* growing on a fouling–release coating.

MATERIALS AND METHODS

In this section turbulent channel flows and boundary layers will be briefly discussed. The purpose is to provide the fundamentals that will be used to relate the two in the subsequent analysis. For a more extensive review, the reader is asked to consult Schlichting (1979) or Schetz (1993). The three methods to relate the results from the turbulent channel flow apparatus to ship scale are then presented. Finally the models are used to predict ship scale detachment of *Enteromorpha* from a fouling-release surface based on laboratory experiments.

Turbulent Channel Flow and Boundary Layer Background

A turbulent channel flow apparatus was designed and constructed to accurately determine the wall shear stress necessary to detach low form fouling from fouling-release surfaces. Details of this design and some preliminary data for the marine diatom *Amphora* settled on glass are given in Schultz *et al.* (2000). There were several reasons why turbulent channel flow was chosen. First, boundary layers around ships and submarines are turbulent. Second, fully-developed channel flows allow accurate determination of the wall shear stress from a relatively simple pressure gradient measurement, as will be subsequently shown. Also, the rectangular cross-section of the channel facilitates the mounting of several replicate microscope slides in the test section.

In order to relate the flow in this device to a ship scale boundary layer, the fundamentals of a fully-developed turbulent channel flow must be understood. Figure 1 shows the development of the boundary layers on the opposite walls of a channel. Fully-developed channel flow occurs downstream of the point where the boundary layers from the opposite walls merge after they have reached a thickness of $H/2$ ($\sim$3.5 mm for the channel of Schultz *et al.*, 2000). For turbulent flow ($Re_H \geq 2,700$), the development length is $\sim 60H$ from the start of the channel (Durst *et al.*, 1998). Downstream of this point, the mean velocity profile and wall shear stress becomes invariant. This condition is termed fully-developed and is illustrated in the control volume shown in Figure 2.

The Reynolds transport theorem for momentum, as given in Equation 1, can be applied to this control volume (Munson *et al.*, 1994).

$$\underbrace{\frac{\partial}{\partial t}\int_{cv}\rho\vec{V}d\forall}_{I} + \underbrace{\int_{cs}\vec{V}\rho(\vec{V}\cdot\vec{n})dA}_{II} = \underbrace{\sum\vec{F}_{CV}}_{III} \qquad (1)$$

Term *I* in Equation 1, represents the rate of change of momentum in the control volume. Since the flow in the channel is steady, this is identically zero. Term *II* represents the net momentum flux through

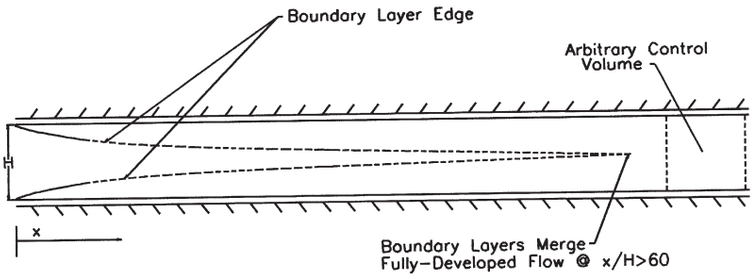

FIGURE 1 Diagram of boundary layer development on the opposite walls of a channel. The flow moves from left to right. A detailed view of the control volume is shown in Figure 2.

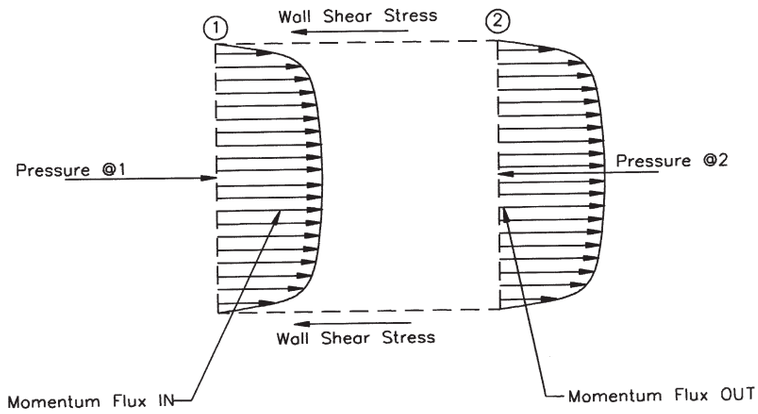

FIGURE 2 Diagram of the control volume in a fully-developed channel flow. Forces act on the top and bottom of the control volume as a result of wall shear stress. Forces act on the right and left sides due to pressure.

Downloaded By: [United States Naval Academy] At: 14:25 21 January 2009

the control surface. Since the flow is fully-developed, the momentum flux into and out of the control volume are equal. Therefore, this term is zero. The result is that the sum of the external forces on the control volume (term *III*) is zero. The external forces acting on the control volume are due to the streamwise pressure gradient and the wall shear stress. Equation 2 shows the balance of these two forces (Hussain & Reynolds, 1975).

$$\tau_w = -\frac{H}{2}\frac{dp}{dx} \tag{2}$$

Using this relationship and a set of calibration runs Schultz *et al.* (2000) derived a formula for the friction factor in their channel (Eqn 3).

$$f = \frac{a}{\mathrm{Re}_H^b} = \frac{0.331}{\mathrm{Re}_H^{0.264}} \tag{3}$$

This friction factor can then be related to the friction velocity and the bulk mean velocity in the channel using Equation (4).

$$\sqrt{\frac{8}{f}} = \frac{\bar{U}}{U_\tau} \Rightarrow U_\tau = \bar{U}\sqrt{\frac{f}{8}} \tag{4}$$

The flow around a ship is marked by a boundary layer that becomes turbulent nearly at the bow and grows in thickness downstream. The boundary layer thickness on a ship may range from ϑ (mm) near the bow to ϑ (m) towards the stern. This is unlike the fully-developed channel flow which has wall shear layers which are a constant thickness of $H/2$ and have a constant wall shear stress at a given flow velocity. Figure 3 shows a typical mean velocity profile in log-normal axes for a turbulent boundary layer. The profile can broadly be divided into two regions, the inner layer and the outer layer. The inner layer occupies the inner 15% of the boundary layer and the outer layer makes up the remainder. Figure 4 compares the ship and laboratory scale shear layer profiles. The profile for the ship scale boundary layer was calculated assuming a zero pressure gradient (*i.e.* a flat plate). Of note is the matching of the mean velocity profiles in the inner layer for the two cases despite the large difference in the overall shear layer thickness. This is because the growth of the boundary layer along a ship occurs primarily in the log-law and outer layer.

Roughness Reynolds Number

For dynamically similar conditions for low form fouling in the channel and on the ship to occur, the ratio of the roughness height, k, to the viscous length scale (ν/U_τ) must be equal for both cases. This parameter is called the roughness Reynolds number and is given by Equation (5).

$$k^+ = \frac{kU_\tau}{\nu} \tag{5}$$

Since the fluid in the channel and for the ship are the same and the height of the fouling organism can be assumed to be the same, ν and k are equal for the ship and channel. Assuming the effects of other flow parameters such as freestream turbulence are negligible, the only parameter that must be matched for dynamic similarity is U_τ. If U_τ is matched, the fouling organism will be exposed to the same mean velocity field and forces in the channel and at ship scale. For the above argument to be valid, the fouling organism must be considered a surface roughness element. This is true if the organism is within the inner layer for both the channel and the ship. Since the boundary layer thickness can reach ϑ (m) on a ship and the inner layer is ~15% of this, macro-fouling organisms like adult barnacles can in many cases be considered surface roughness. In the channel flow device of Schultz *et al.* (2000), the inner layer thickness is ~0.53 mm. Organisms larger

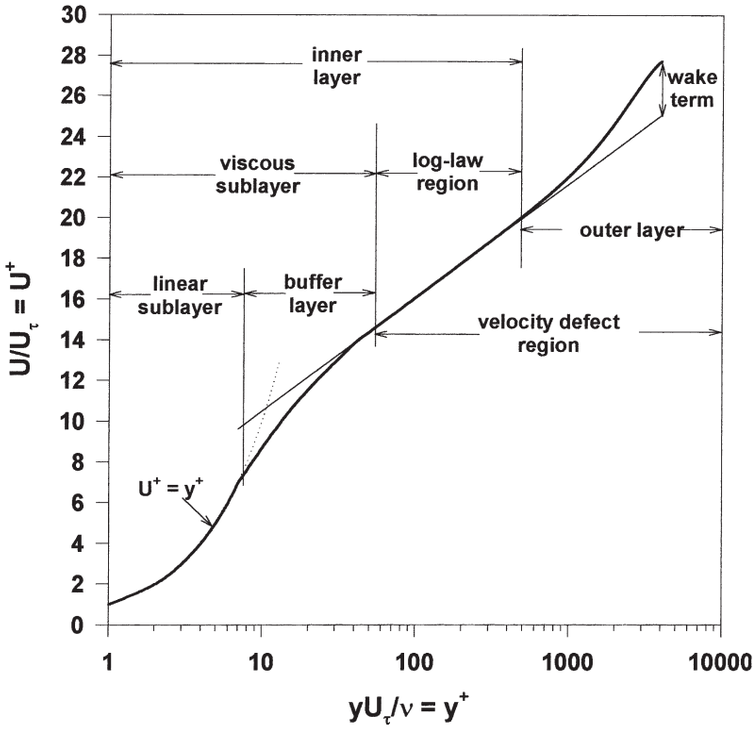

FIGURE 3 Normalized mean velocity profile in a turbulent boundary layer in semi-log coordinates. Illustrated are the various layers that make up the boundary layer.

Downloaded By: [United States Naval Academy] At: 14:25 21 January 2009

than this will extend into the outer layer where the velocity profiles and subsequently the forces will become different from that at ship scale. This can be seen in Figure 4 where the velocity profiles do not match in the outer layer. However, as long as the organism is less than the inner layer height of the channel, dynamic similarity with ship scale can be achieved. Since this involves matching U_τ, three methods of calculating this parameter at ship scale will be presented.

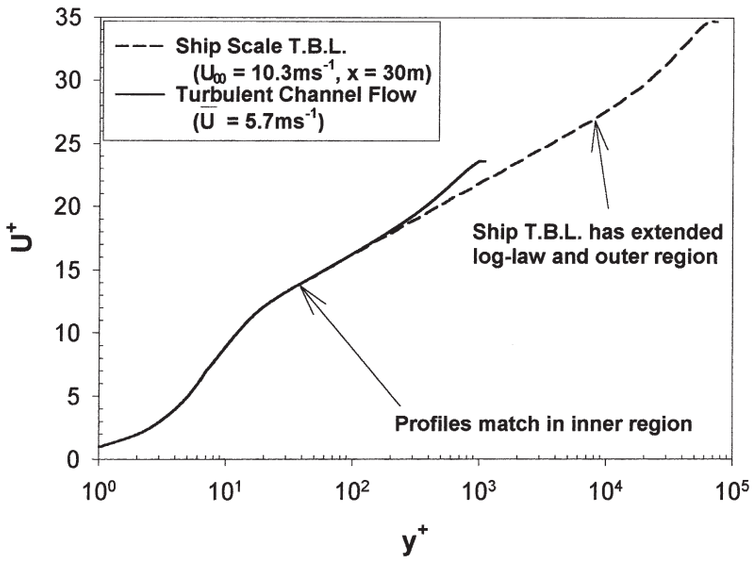

FIGURE 4 Comparison of the mean velocity profiles in a ship scale boundary layer and a turbulent channel flow. Note the overlap of the two that extends to the outer edge of the inner layer of the channel flow.

Downloaded By: [United States Naval Academy] At: 14:25 21 January 2009

Power Law Model

One of the simplest calculation methods to predict U_τ at ship scale is to use a power law formula. In this case the ship is modelled as a smooth planar surface. While ships are strictly neither smooth nor planar, this analysis should provide a reasonable approximation. The local skin–friction coefficient can be calculated using the power law formula given by Schlichting (1979).

$$c_f = \frac{0.02296}{\mathrm{Re}_x^{0.139}} \tag{6}$$

The friction velocity at ship scale can then be related to the local skin friction coefficient and the free-stream velocity using Equation 7.

$$\sqrt{\frac{2}{c_f}} = \frac{U_\infty}{U_\tau} \Rightarrow U_\tau = U_\infty \sqrt{\frac{c_f}{2}} \tag{7}$$

ITTC-57 Model

Another calculation method to predict U_τ at ship scale is to use the ITTC-57 ship-model correlation formula for the frictional resistance coefficient (Lewis, 1988). Again the ship is modelled as a smooth planar surface. The ITTC-57 formula is given as:

$$C_F = \frac{0.075}{(\log_{10}\mathrm{Re}_L - 2)^2} \tag{8}$$

The local skin–friction coefficient at a position $x = L$ can be found using the similarity analysis formula of Granville (1958) as:

$$\sqrt{\frac{c_f}{2}} = \frac{U_\tau}{U_\infty} = \sqrt{\frac{C_F}{2}}\left(1 - \frac{1}{\kappa}\sqrt{\frac{C_F}{2}}\right) \tag{9}$$

Equations 8 and 9 can then be iteratively solved to obtain U_τ at ship scale.

Computational Fluid Dynamics (CFD) Model

The final calculation method used in the present investigation to predict U_τ at ship scale is a computational fluid dynamics (CFD) model. The CFD program used is a two-dimensional, implicit, incompressible, turbulent boundary layer code to solve the Reynolds-averaged Navier–Stokes equations (RANS). The turbulence model is a Van Driest mixing length model. Details of the computational code and the turbulence model are given in Schetz (1993). In order to incorporate the effect of streamwise pressure gradient (*i.e.* hull curvature) into the calculation, the pressure distribution around the *Lucy Ashton*, a modified British paddle steamer on which a great deal of hydrodynamic data have been collected, is used. The ship measures 58 m in length and has a displacement of 397 metric tons. Further details of the ship are given in Anon (1952).

Experimental results for the static pressure distribution on a scale model of the *Lucy Ashton* collected by Smits (1982) and Smits and Joubert (1982) along the mid streamline were used. The variation of the pressure coefficient along the length of the model is shown in Figure 5. A total of 10^5 points

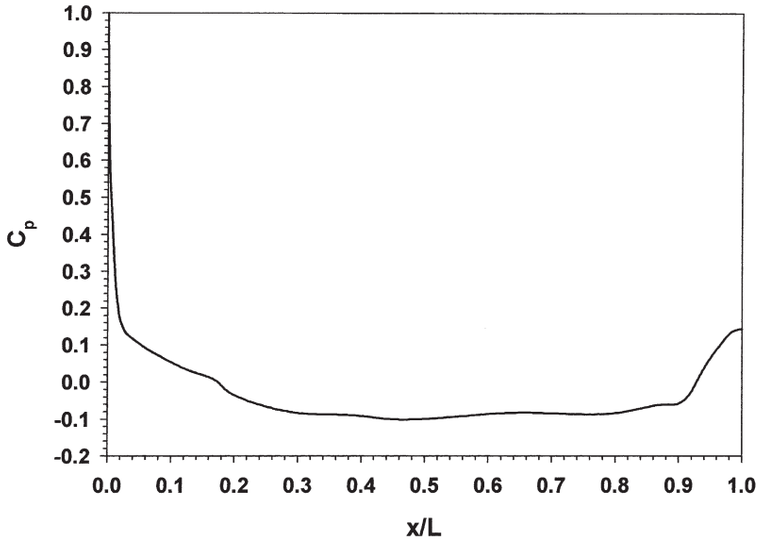

FIGURE 5 Coefficient of pressure *vs* streamwise distance for the *Lucy Ashton* from Smits (1982) and Smits and Joubert (1982). Data were collected on a scale model on the mid-streamline.

Downloaded By: [United States Naval Academy] At: 14:25 21 January 2009

in the wall-normal direction and 2000 streamwise locations were used for the CFD calculation (2×10^8 total grid points). The results were checked to ensure that the solution was grid independent. The boundary layer was assumed to be turbulent from the leading edge and no transition model was used. The CFD calculation was made for $1\,\mathrm{m\,s^{-1}} \leq U_\infty \leq 13\,\mathrm{m\,s^{-1}}$.

Algal Experiments

Zoospores were released from fertile *Enteromorpha* plants as described in Callow *et al.* (1997). Spore suspensions (10 ml, 1.5×10^6 spores $\mathrm{ml^{-1}}$) were added to individual compartments of polystyrene culture dishes (In Vitro Systems & Services, GmbH) each containing a test surface. The spores were allowed to settle in the dark for 2 h before being washed gently to remove unattached spores. The slides were transferred to clean dishes and incubated in Provasoli's ES enriched seawater (Starr & Zeikus, 1987) that was changed after 3 d, in a growth cabinet (Sanyo MLR-350) at 18°C with a 16:8 light:dark cycle (photon flux density 330 $\mu\mathrm{mol\,m^{-2}\,s^{-1}}$). Biomass was quantified by extraction of chl *a* into dimethyl sulphoxide (DMSO) as described by Jeffrey and Humphrey (1975).

Test surfaces were acid-washed glass microscope slides and glass slides coated with Veridian (International Paint fouling-release yacht product). Spores were settled onto 18 replicates of each surface. At each time point, 3 replicate slides were treated as follows. The algal biofilm was scraped from half of the area of each slide into a tube for extraction of chlorophyll. The strength of adhesion of the remaining algal biofilm was examined using the turbulent channel flow apparatus described in Schultz *et al.* (2000), fitted with a higher capacity pump. Colonised surfaces were challenged at the highest flow rate of 212 l $\mathrm{min^{-1}}$ ($\bar{U} = 4.7\,\mathrm{ms^{-1}}$), equivalent to a wall shear stress of 56 Pa, for 5 min. The slides were positioned such that the biofilmed area was at the leading edge of flow. Biomass remaining was determined as described above. The percentage of biofilm remaining after flow was calculated for each time point. Measurement of the length of the algal filaments was made on the 6 d samples.

RESULTS AND DISCUSSION

By substituting the power law formula for a flat plate boundary layer (Eqn 6) into Equation 7 and rearranging, the following formula relating U_∞ to U_τ at ship scale results:

$$U_\infty = \left(9.333 U_\tau \left(\frac{x}{\nu}\right)^{0.0695}\right)^{1.0747} \tag{10}$$

Equation 10 can be solved to find the ship speed (U_∞) at which there is dynamic similarity with the channel flow apparatus at an equivalent value of U_τ for any downstream distance (x).

In a similar way, substituting the ITTC-57 formula for frictional resistance coefficient (Eqn 8) into Equation 9 and rearranging, a formula relating U_∞ to U_τ at ship scale may also be obtained:

$$U_\infty = U_\tau \sqrt{\frac{2}{\left(0.075/\left(\log_{10}\left(\frac{U_\infty x}{\nu}\right) - 2\right)^2\right)}} \times \left(1 - \frac{1}{\kappa}\sqrt{\frac{\left(0.075/\left(\log_{10}\left(\frac{U_\infty x}{\nu}\right) - 2\right)^2\right)}{2}}\right)^{-1} \tag{11}$$

Equation 11 can be solved iteratively to find the value of U_∞ at which there is dynamic similarity with the channel flow apparatus at an equivalent value of U_τ for any x.

The CFD model was also used to calculate U_τ as a function of U_∞ and x for the *Lucy Ashton*. The results of all three models at various downstream distances are presented in Figures 6–10. For these results, the working fluid was assumed to be seawater at 15°C ($\nu = 1.188 \times 10^{-6}\,\mathrm{m^2\,s^{-1}}$, $\rho = 1026\,\mathrm{kg\,m^{-3}}$), and calculations were made using the calibration constants for the channel flow device at the University of Birmingham (Eqn 3) of $a = 0.331$ and $b = 0.264$. It should be noted that the maximum value of $\bar{U}$ for the Birmingham channel is $4.7\,\mathrm{m\,s^{-1}}$. However, the calculations presented in Figures 6–10 were carried out for $\bar{U}$ up to $7.0\,\mathrm{m\,s^{-1}}$. This corresponds to the maximum $\bar{U}$ for a newer version of the turbulent channel flow apparatus presently in use at the University of Hawaii.

Of note is the excellent agreement between the results for the power law and the ITTC-57 formulae. The predictions are within ±1% throughout the entire velocity range for all downstream distances. The CFD results for $x = 1$ m agree with the other two methods within 2%. For the downstream distances $x = 5, 10$, and 25 m the agreement gets systematically worse. This can be explained by looking at Figure 5. The value of C_p in this range is dropping, indicating a favorable pressure gradient. This leads to an increase in U_τ at a given value of U_∞ compared to a zero pressure gradient flow (*i.e.* a flat plate). The results are in better agreement at $x = 50$ m. By this location the value of C_p is increasing, indicating an adverse pressure gradient. This leads to a decrease in U_τ and better agreement with the flat plate results. It is of note that the results for all the methods agree within 15% over the entire range of x and U_∞, and the agreement is generally much better than this. The differences observed between CFD model and

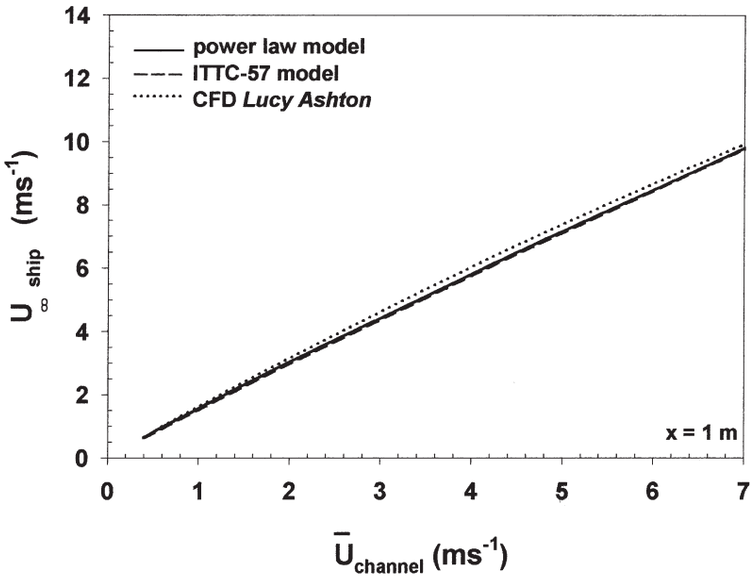

FIGURE 6 Ship velocity *vs* bulk velocity mean to achieve equivalent friction velocity. Results for 1 m downstream of the leading edge.

the other two are primarily a result of the streamwise pressure gradient applied in the CFD model, which is absent in the flat plate models. It should be noted that streamwise pressure gradient can vary considerably for one hull form to another.

Algal Experiments

The number of spores that attached on the two types of test surface had been found in a number of experiments not to be significantly different (data not shown). Growth of sporelings on glass and the Veridian coating was not significantly different except at 4 and 5 days (Figure 11), when a higher amount of biomass was recovered from the Veridian coatings. After 6 d, most of the spores had germinated on both types of surface with a mean filament length of 85.0 ± 8.8 μm on glass. In other experiments, the length of sporelings on glass and Veridian has been shown not to be significantly different. It should be stated that after 6 d of growth the length of the sporelings remained less than the inner layer thickness (0.53 mm) in the channel. This means that the sporelings can be considered a surface roughness and similarity scaling can be used. This is not to say that the attached spores will not

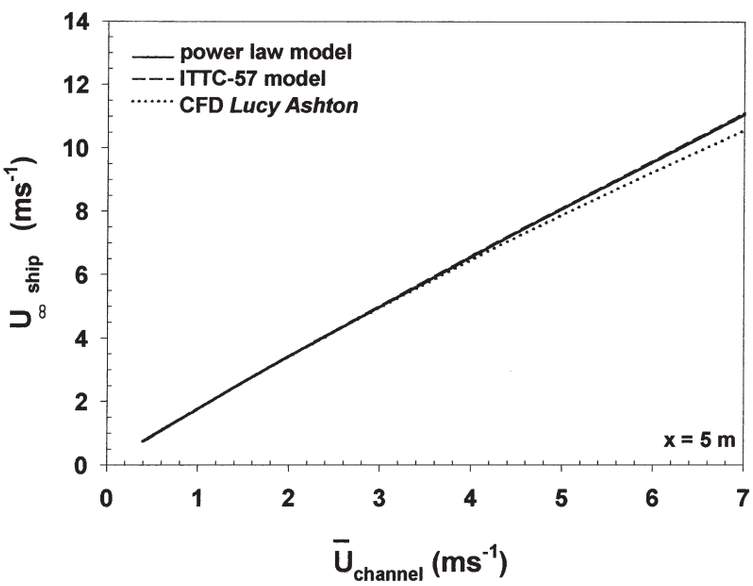

FIGURE 7 Ship velocity *vs* bulk velocity mean to achieve equivalent friction velocity. Results for 5 m downstream of the leading edge.

Downloaded By: [United States Naval Academy] At: 14:25 21 January 2009

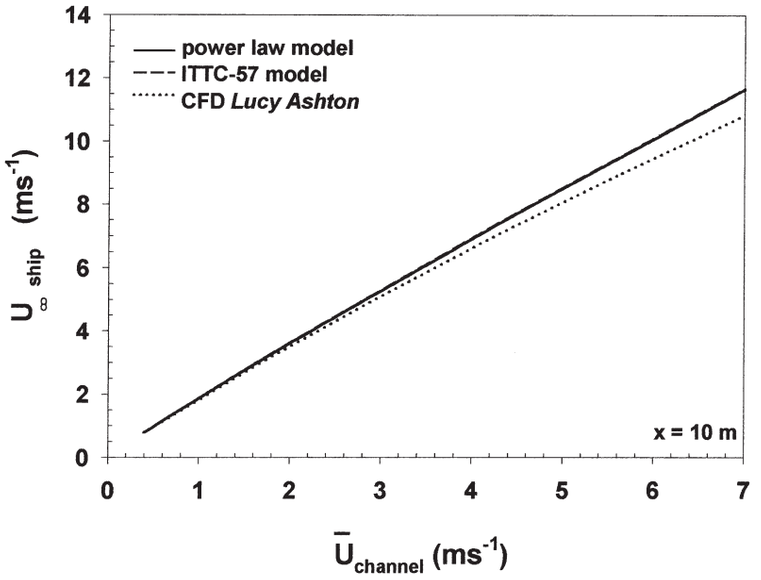

FIGURE 8 Ship velocity *vs* bulk mean velocity to achieve equivalent friction velocity. Results for 10 m downstream of the leading edge.

affect the wall shear stress in the channel. They most certainly will increase it, and the increase will be likely to be greater as the sporelings grow. However, a concomitant increase in wall shear stress should also occur in the turbulent boundary layer on a ship due to the attached sporelings.

On glass, 30% or less of the biofilm was removed at all time points over the 6 d of the experiment, and an age-related trend was not apparent (Figure 12). In contrast, the percentage removal of the biofilm from the Veridian coating increased with biofilm age, and after 5 d growth approximately 80% was removed. Since the length of sporelings on glass and Veridian was not significantly different, the enhanced removal from Veridian is attributed to its fouling-release properties. These results indicate that while the shear stress on the biofilm most likely increases as it grows on both substrata, the adhesion strength must also increase at a similar rate on glass, while on the Veridian it stays the same or decreases, leading to increased removal over time. Using these experimental results as inputs to the three models developed here, >60% removal of a 4–6 d old *Enteromorpha* biofilm from a ship coated with Veridian could be expected at downstream distance of 50 m at a ship velocity of 9.1 m s^{-1} (17.7 knots),

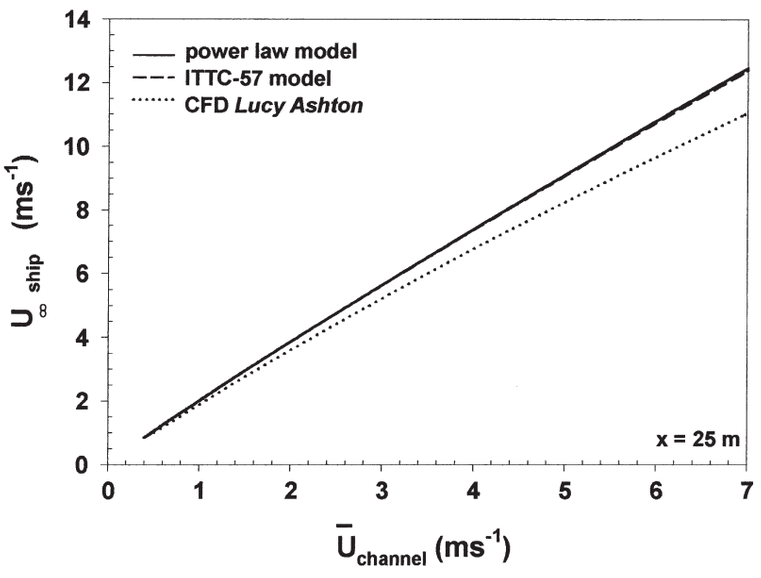

FIGURE 9 Ship velocity *vs* bulk mean velocity to achieve equivalent friction velocity. Results for 25 m downstream of the leading edge.

Downloaded By: [United States Naval Academy] At: 14:25 21 January 2009

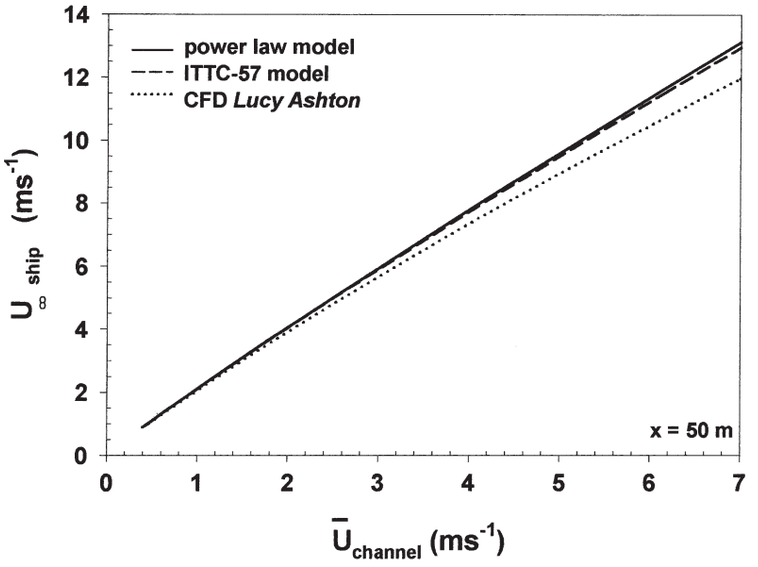

FIGURE 10 Ship velocity *vs* bulk mean velocity to achieve equivalent friction velocity. Results for 50 m downstream of the leading edge.

Downloaded By: [United States Naval Academy] At: 14:25 21 January 2009

$9.0\,\mathrm{m\,s^{-1}}$ (17.5 knots), and $8.4\,\mathrm{m\,s^{-1}}$ (16.4 knots) using the power law, ITTC-57, and CFD models respectively. Less than 30% removal of the same age biofilm can be expected on a glass surface at the same velocities.

CONCLUSIONS

Three models to relate the detachment of low form fouling at laboratory and ship scale have been developed. The overall agreement between the three methods is good. These models provide a framework from which to relate the performance of fouling-release surfaces in laboratory assays to the actual self cleaning of a ship. The results indicate that significant removal of 4–6 d old *Enteromorpha* biofilms can be expected at operationally relevant ship velocities on the Veridian fouling-release surface. While the present models were produced to relate results from the turbulent channel flow apparatus of Schultz *et al.* (2000) to ship boundary layers, a similar procedure could be used for other hydrodynamic assays. Further research including full scale ship trials is needed to better assess the accuracy of the models and to allow better prediction of the performance of fouling-release surfaces.

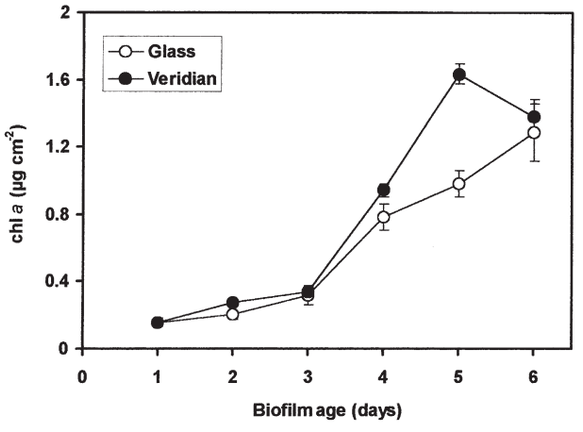

FIGURE 11 Growth of *Enteromorpha* biofilm on glass (○) and Veridian (●). Biomass was measured by extraction of chl *a*. Points are the mean of 3 replicates; bars = 95% confidence limits.

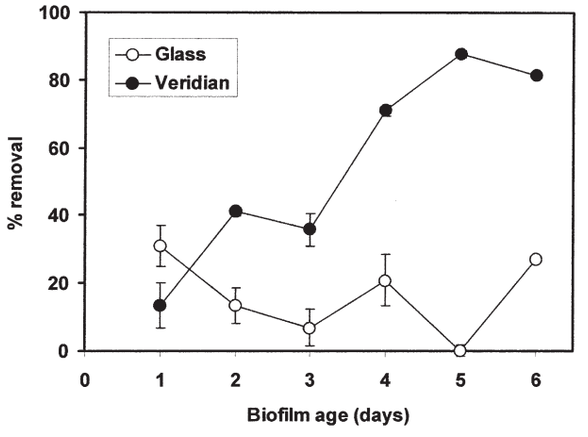

FIGURE 12 Percentage removal of *Enteromorpha* biofilm from glass (○) and Veridian (●) at a wall shear stress of 56 Pa. Biomass was measured as chl *a*. Percentage removal was calculated from 3 replicate slides exposed to flow compared to control slides not exposed to flow. Bars = 95% confidence limits from arcsine transformed data.

Acknowledgements

The authors gratefully acknowledge the support of this research by the Office of Naval Research through awards N0001401WR20339 to MPS and N00014-99-1-0311 to JAC/MEC. Thanks are also given to Professor Steve Miner who assisted with the CFD work and to Dr David Williams (Akzo-Nobel, Felling UK) who provided the glass slides coated with Veridian.

References

Anon (1952) Resistance tests on the *Lucy Ashton*, Part I—Naked hull conditions. Report #107. British Shipbuilding Research Association, London

ASTM D5618 (1994) Standard test method for the measurement of barnacle adhesion strength in shear. ASTM 6.01

Callow M E, Callow J A, Pickett-Heaps J D, Wetherbee R (1997) Primary adhesion of *Enteromorpha* (Chlorophyta, Ulvales) propagules: quantitative settlement astudies and video microscopy. *J Phycol* **33**: 938–947

Durst F, Fischer M, Jovanovic J, Kikura H (1998) Methods to set up and investigate low Reynolds number, fully developed turbulent plane channel flows. *ASME J Fluids Eng* **120**: 496–503

Finlay J A, Callow M E, Schultz M P, Swain G W, Callow J A (2002) Adhesion strength of settled spores of the green alga *Enteromorpha*. *Biofouling* **18**: 251–256

Granville P S (1958) The frictional resistance and turbulent boundary layer of rough surfaces. *J Ship Res* **2**: 52–74

Hussain A K M F, Reynolds W C (1975) Measurements in fully developed turbulent channel flow. *ASME J Fluids Eng* **97**: 568–580

Jeffrey S W, Humphrey G F (1975) New spectrophotometric equations for determining chlorophylls a, b, c1 and c2 in higher plants, algae and natural phytoplankton. *Biochem Physiol Pflanz* (BPP) **167**: 191–194

Kovach B S, Swain G W (1998) A boat-mounted foil to measure the drag properties of antifouling coatings applied to static immersion panels. *Proc Int Symp Seawater Drag Reduction*, Newport, RI: 568–580

Lewis E V (ed) (1988) *Principles of Naval Architecture*, Volume II, 2nd Edition. SNAME, Jersey City, New Jersey

Munson B R, Young D F, Okiishi T H (1994) *Fundamentals of Fluid Mechanics*, 2nd Edition. John Wiley & Sons, New York

Schlichting H (1979) *Boundary-Layer Theory*, 7th Edition. McGraw-Hill, New York

Schetz J A (1993) *Boundary Layer Analysis*. Prentice-Hall, Englewood Cliffs, New Jersey

Schultz M P, Finlay J A, Callow M E, Callow J A (2000) A turbulent channel flow apparatus for the determination of the adhesion strength of microfouling organisms. *Biofouling* **15**: 243–251

Smits A J (1982) Turbulence stimulation and the initial boundary-layer development on two ship forms. *J Ship Res* **26**: 166–175

Smits A J, Joubert P N (1982) Turbulent boundary layers on bodies of revolution. *J Ship Res* **26**: 135–147

Starr R C, Zeikus J A (1987) UTEX—The culture collection at the University of Texas. *J Phycol* **23**(suppl.):S1–S27

Swain G W, Schultz M P (1996) The testing and evaluation of non-toxic antifouling coatings. *Biofouling* **10**: 187–197

Swain G W, Nelson W G, Preedeekanit S (1998) The influence of biofouling and biotic disturbance on the development of fouling communities on non-toxic surfaces. *Biofouling* **12**: 257–269

Downloaded By: [United States Naval Academy] At: 14:25 21 January 2009